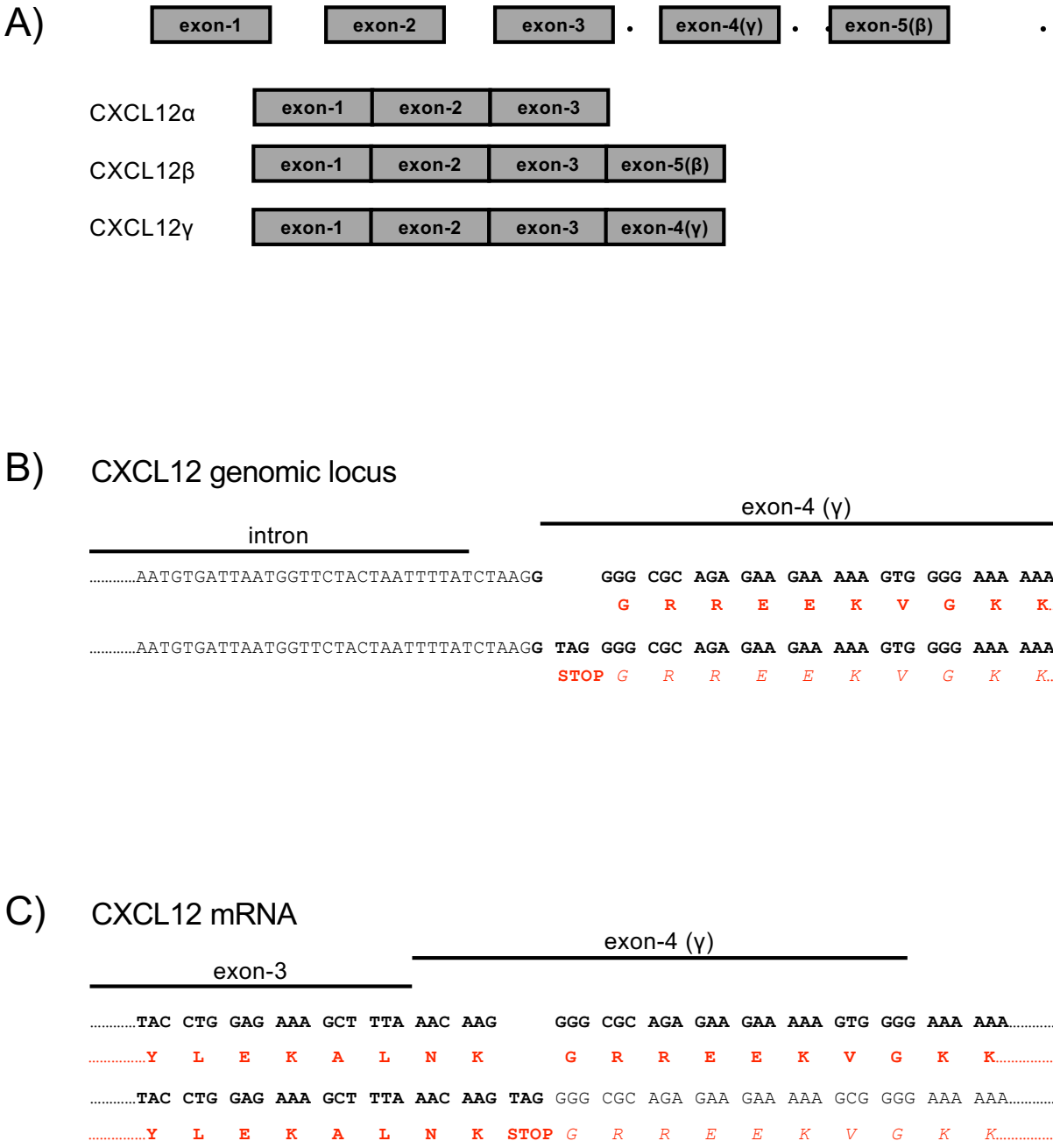

Figure S1: Generation of a CXCL12γ-deficient mouse line

(A) *Schematic representation of the genomic Cxcl12 locus organization (top) and corresponding mature mRNA splice variants (bottom).*

(B) *Nucleotide sequence alignment of the intron/exon 4 junction in CXCL12^{WT} and CXCL12$^{\Delta\gamma}$ genomes. The corresponding amino acid sequence is shown in red. Introduction of a premature stop codon at the intron/exon 4 junction in CXCL12$^{\Delta\gamma}$ mice prevents translation of exon 4 (italicized red letters), resulting in production of the CXCL12α isoform.*

(C) *Nucleotide sequence comparison of the exon 3/exon 4 junction in CXCL12^{WT} and CXCL12$^{\Delta\gamma}$ spliced mRNAs. The engineered stop codon is positioned at the exon 3/exon 4 junction following splicing. The CXCL12γ C-terminal domain, encoded by exon 4, is present in CXCL12^{WT} mice (red letters) but absent in CXCL12$^{\Delta\gamma}$ mice (italicized red letters).*

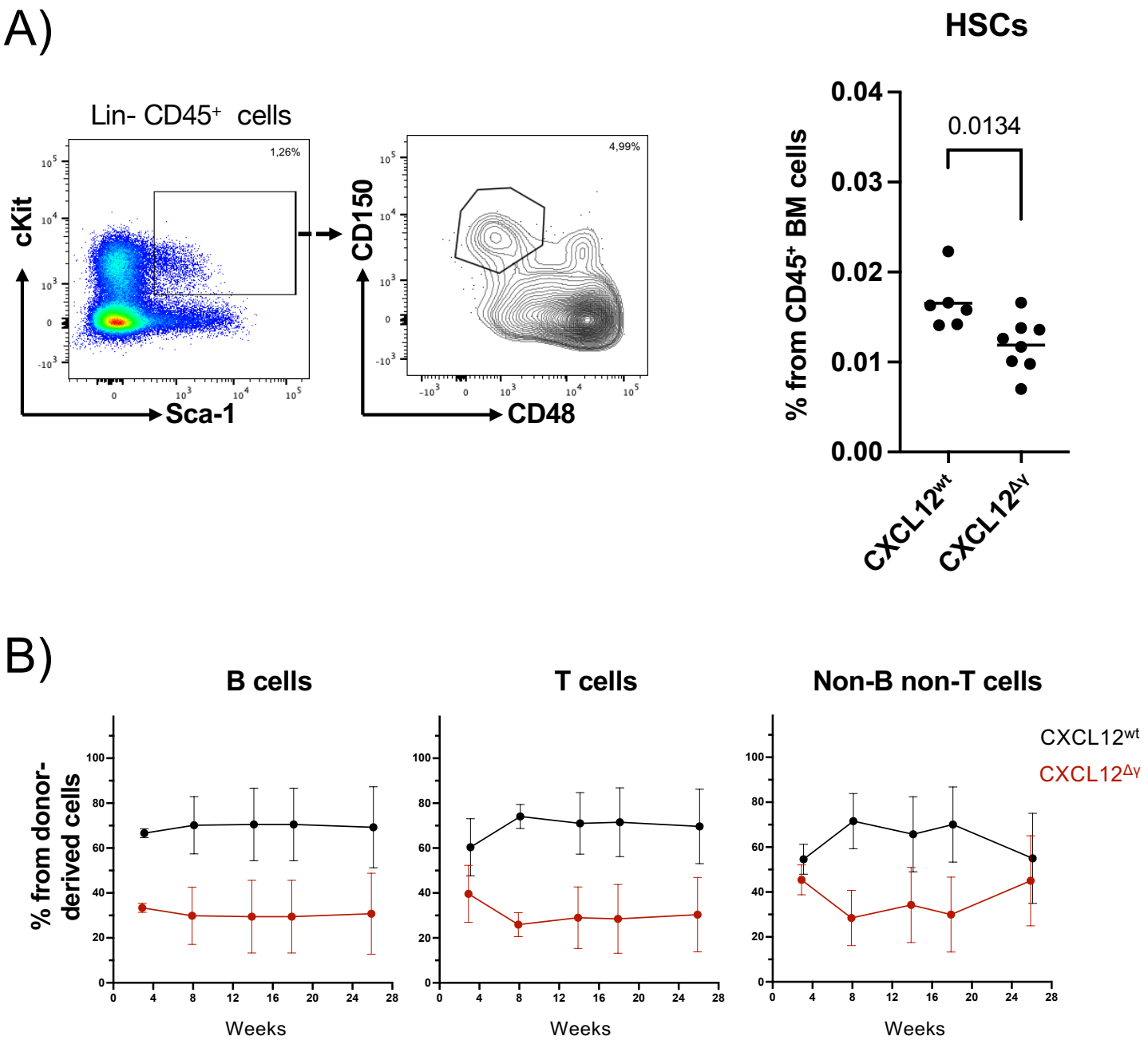

Figure S2: CXCL12γ controls the hematopoietic stem cell population size in bone marrow

(A) *Left: Flow cytometry gating strategy for identification of bone marrow hematopoietic stem cells (HSCs; Lin$^-$Sca-1$^+$c-Kit$^+$CD48$^-$CD150$^+$). Right: Quantification of HSCs as percentage of CD45$^+$ cells in CXCL12^{wt} and CXCL12$^{\Delta\gamma}$ mice.*

(B) *Kinetics of donor-derived (CD45.2$^+$) hematopoietic reconstitution in competitive bone marrow transplantation experiments. Shown are B cells (CD19$^+$B220$^+$), αβ T cells (CD3$^+$TCRβ$^+$), and non-B non-T cells at indicated time points post-transplantation in recipients of CXCL12^{wt} or CXCL12$^{\Delta\gamma}$ bone marrow cells.*

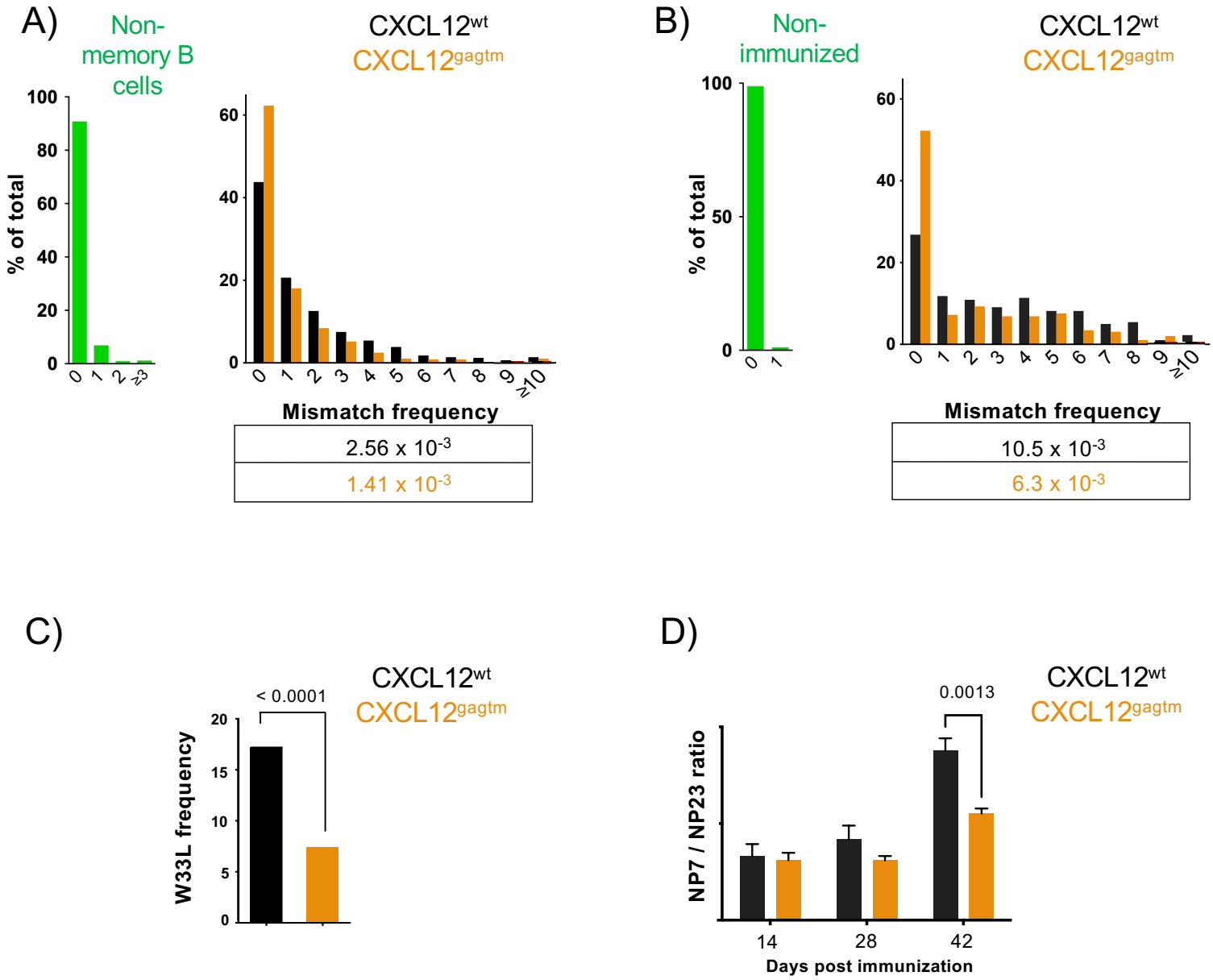

Figure S3: Impaired antibody affinity maturation in CXCL12^{gagtm} mice

(A) *Somatic hypermutation analysis in memory B cells of CXCL12^{gagtm} mice. AID-Cre × ROSA-lox-YFP reporter mice allow identification of cells with past GC experience. Mutation frequency distributions in the J_H4 intron are shown for naive B cells (CD19$^+$IgD^{hi}CD95$^-$CD38$^+$YFP$^-$) isolated from one AID-Cre × ROSA-lox-YFP mouse (left panel), and memory B cells (CD19$^+$IgD$^-$CD95$^-$CD38$^+$YFP$^+$) from 4 pooled wild-type and 4 pooled CXCL12^{gagtm} recipient mice (right panel). The table shows mutation frequencies as percentage of total analyzed nucleotides.*

(B) *Somatic hypermutation following primary T cell-dependent immunization of CXCL12^{gagtm} mice. Mutation frequency distributions in the V_H186.2 gene are shown for naive IgD^{hi} B cells (left panel) and λ1$^+$ GC B cells (CD19$^+$IgD$^-$CD38$^-$CD95$^+$) from 5 pooled wild-type and 5 pooled CXCL12^{gagtm} mice (right panel). The table shows mutation frequencies as percentage of total analyzed nucleotides.*

(C) *Frequency of W33L substitutions in VH186.2 sequences from experiments in (B). Statistical significance determined by Fisher's exact test.*

(D) *Affinity maturation assessed by NP^7/NP^{23}-specific IgG1 titer ratios in sera collected at indicated time points following NP^{16}-CGG immunization of 2 wild-type and 6 CXCL12^{gagtm} mice.*

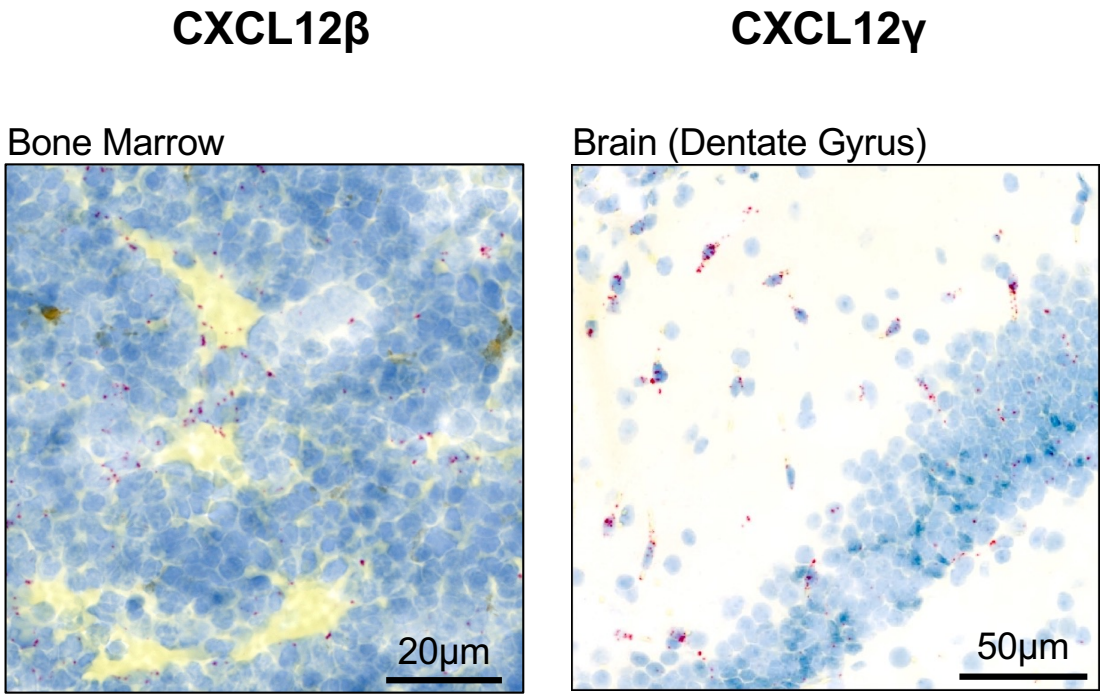

Figure S4: CXCL12β and CXCL12γ isoforms expression in bone marrow and brain

Positive control showing robust detection of Cxcl12β transcripts in bone marrow (left) and Cxcl12γ transcripts in the brain dentate gyrus (right), confirming BaseScope probe specificity and sensitivity.